JOURNAL OF CATALYSIS 120, 137–156 (1989)

The CO/H_2 Reaction on Rh/Al_2O_3

II. Kinetic Study by Transient Isotopic Methods

ANGELOS M. EFSTATHIOU AND CARROLL O. BENNETT

Department of Chemical Engineering, University of Connecticut, Storrs, Connecticut 06268

Received January 10, 1989; revised May 3, 1989

Transient isotopic methods have been used to study the CO/H_2 reaction over 5% Rh/Al_2O_3 in the temperature range 180–260°C. The steady-state tracing method permits the determination of the surface coverage of CO and active carbon C_α during reaction, without the need for quenching in helium and subsequent titration by hydrogen. The results confirm that the sequence of steps for methane formation passes through a small reservoir of active carbon ($\theta_{C_\alpha} < 0.05$), although there is also a large reservoir of surface CO. Rate control is largely determined by the rate of CO dissociation on the surface. The simultaneous presence of a formate species, located on the alumina and which does not participate in the reaction, has been supported by the results of isotopic experiments.

INTRODUCTION

In Part I of this study (*1*) certain transient methods were used to estimate the composition of the surface of a 5% Rh on alumina catalyst during the methanation reaction. These procedures involve a switch of the feed from the H_2/CO mixture to pure H_2, so that the surface species are titrated, principally to methane, after the reaction has been quenched. In particular it has been necessary to assume that the CO coverage during the reaction in H_2/CO is the same as that found by a titration following the passage of He/CO through the reactor.

In the present study the surface coverage of CO during the reaction will be obtained by the method of steady-state tracing (*2–4*), which involves a switch of the reactor feed from $H_2/^{12}CO$ to $H_2/^{13}CO$ and the observation of the response of ^{13}CO and $^{13}CH_4$ at the reactor outlet. Except for the identity of the carbon isotope, the composition of the catalyst surface remains constant, leading to a truly *in situ* estimation of the surface coverages.

In the steady-state tracing, the CO coverage is obtained from the ^{13}CO response, and the active carbon C_α coverage from the $^{13}CH_4$ response. The C_α coverage in Part I was estimated from a temperature programed reduction obtained after quenching the H_2/CO reaction by a switch to He. The tracing experiment probes for the quantity of C_α intermediate which participates directly in the sequence of steps, whereas some of the carbon species measured by titration may be merely spectator species (*5*).

A direct switch from H_2/CO to H_2 at reaction temperature leads to the isothermal titration of all the surface carbon-containing species at low temperature and short time in the reaction mixture (e.g., 180°C and 2 min). However, for higher temperatures and longer times a temperature programed reduction (TPR) after the isothermal reduction leads to additional methane production, arising from less reactive species: a formate, and a less reactive carbon called C_β (*1*). More precisely, methane produced at $T > 350$°C is defined as representing C_β. Finally, surface formate residing on the Al_2O_3 has been estimated by the difference relation, $\theta_{COOH} = \theta_{CS} - \theta_{CO} - \theta_{C_\alpha} - \theta_{C_\beta}$, where θ_{CS} is the total coverage of carbonaceous species from the isothermal reduction plus the TPR.

0021-9517/89 $3.00

The assignment of the extra carbonaceous species as described above to surface formate is based principally on the work of Solymosi and his students (*6–8*). They have found by infrared studies that formate species (strong bands at 1590 and 1380 cm^{-1}) form during the methanation reaction on supported Rh catalysts, including Rh/Al_2O_3. Similar bands have been observed for Ru/Al_2O_3 (*9*) and Ni/Al_2O_3 (*4*). The same bands form slowly from CO on Al_2O_3 alone (*10, 11*) or immediately when HCOOH(g) is passed over Rh/Al_2O_3 or Al_2O_3 alone (*6*). In what follows, we shall use some isotopic methods to probe for the presence of formate during reaction and to decide whether it is a reaction intermediate or a spectator.

The amounts of surface carbon of various types which accumulate during reaction increase dramatically with temperature, as found in Part I (*1*) and also by Orita *et al.* (*12*). At 260°, the highest temperature used in the present work, it appears that at least one more form of carbon exists in addition to C_α and C_β at times on stream greater than 30 min.

The role of the support in changing the activity of the H_2/CO reaction over supported Rh has been studied (*7, 12*). The activities (methane is the main product) can be ranked according to the supports, as follows: $TiO_2 > Al_2O_3 > SiO_2 > MgO$. Formate accumulates on alumina and magnesia but not on silica (*7*). A goal of the present work is to determine with some precision the surface state of the metal and support during reaction in the hope that the results will lead to a better understanding of the support effects. We plan later to study $Rh/Mg(OH)_2$, Rh/La_2O_3, and $LaRhO_3$ catalysts, which exhibit higher selectivity toward oxygenated products.

EXPERIMENTAL

The general methods used in this work have already been described (*1, 4*). Here we give some details which apply particularly to the experiments involving isotopes.

Isotopic mixtures. All the H_2/CO and He/CO mixtures used here are 9.9 mol% CO, where the CO has the isotopic composition described in what follows. The H_2/CO mixture was made from a lecture bottle of ^{13}CO which was 91.71% ^{13}CO (Matheson). To save isotopic gas and to keep the mass spectrometer detection system (*1*) in the linear range for ^{13}CO, the gases H_2, ^{12}CO, and ^{13}CO were combined so that the 9.9% overall CO mixture had a ^{13}C content of 54.9%. The $^{13}C^{16}O$ gas used contained $^{12}C^{17}O$ as an impurity, and the signal at $m/e = 29$ was used to monitor the $^{13}C^{16}O$. The results of the CO exchange experiments were corrected for the known concentrations of the various isotopes in the purchased ^{13}CO as well as for the natural abundance (1.1%) of ^{13}CO in ordinary CO. One percent Ar was also added to the $H_2/^{13}CO$ to facilitate obtaining the forcing and mixing curves (*4*) needed to interpret the steady-state tracing experiments.

In certain exchange experiments, the interpretation of the results is facilitated if all the initial surface ^{12}CO is exchanged by ^{13}CO. For this purpose a He/CO mixture has been prepared in which the CO is 99.3% ^{13}C. The CO was obtained from a lecture bottle of CO also having a ^{13}C content of 99.3%.

Mass spectrometry. For the measurement of the response of $^{13}CH_4$ in the steady-state tracing experiments, the peak at $m/e = 17$ has been followed. $^{12}CH_4$ was followed by measuring the peak at $m/e = 15$. Since water is being produced in these experiments, it is convenient to tune the mass spectrometer to a resolution of 600 so that the $^{13}CH_4$ peak is separated from the OH^+ peak. In the absence of $^{13}CH_4$, there was no contribution from the OH^+ peak at the m/e corresponding to $^{13}CH_4$. Careful cleaning eliminated a problem which had been caused by NH_3^+, probably generated over the iron catalyst of that study (*5*).

Since we had no pure $^{13}CH_4$ from which to measure its cracking pattern, the contribution of $^{13}CH_4$ to the 15 peak was mea-

sured by using the known mixture of H_2/^{12}CO/^{13}CO which has been described above. Measurement of the total CH_4 at steady-state by chromatography (FID) along with the 15 and 17 peaks obtained by reaction permitted the required information to be deduced. For the ion-source conditions used, the intensity ratio of the peaks 15/17 for $^{13}CH_4$ was found to be 0.14.

For the measurement of CO ($m/e = 28$) in the presence of CO_2, the contribution of the CO_2 to the 28 peak was found to be such that the intensity ratio 28/44 for CO_2 was 0.12.

In order to measure the isothermal desorption of CO during the switch from H_2/CO to pure H_2, it was necessary to follow the 28 peak as the CO content decayed from 9.9% toward zero. Since the initial CO concentration was beyond the linear range of the electron multiplier/electrometer detection system of the mass spectrometer, a calibration curve (28 signal/concentration) was prepared.

Remarks on the reactor. Although the reactor and its behavior have already been discussed (*1, 4*), a few pertinent points are recalled here. For the experiments of this study, 30 mg of catalyst is held on a very fine stainless steel screen to form a shallow bed of about 7 mm diameter in the reactor space (0.5 ml) which is located between the small passages (1.5 mm diameter) leading to and from the reactor. With the experimental flow rate of 30 ml/min, the value of the Peclet number for mass transport is less than unity, based on molecular diffusion. Since the turbulence introduced at the gas entrance is appreciable, the actual eddy diffusion is considerably greater than the molecular value. In other words, the mass transport by axial dispersion overwhelms the transport by the net flow through the reactor. Thus the reactor is expected to approximate a single stirred tank. Channeling is irrelevant in such a reactor. It is therefore not surprising that switching experiments using inert gases (*4*) agree with the behavior of a well-mixed reactor.

The catalyst particles used are formed by breaking up a disk of about 0.2 mm thickness made by pressing the original Rh/Al_2O_3 powder (*1*). The Thiele modulus is thus so small that no diffusional resistances are expected.

RESULTS

Steady-state tracing. Figure 1 shows the response of the reactor outlet composition after the sequence He(180s) $\rightarrow$ ^{12}CO/H_2(120s) $\rightarrow$ ^{13}CO/H_2(t) at 220°C. The results are expressed in terms of the variable Z, which represents the fraction of the ultimate change (giving $Z = 1$) as a function of time. Thus Z is defined by

$$Z(t) = (y(t) - y_0)/(y_\infty - y_0), \qquad (1)$$

where the subscripts 0 and ∞ refer to values of y (mole fraction) just before the switch ($t = 0$) and long after the switch ($t \rightarrow \infty$). The curve F (forcing) is obtained from the argon response ($y_0 = 0$, $y_\infty = 0.01$) as the gas flows through a bypass around the reactor. The curve M (mixing) is the response of the argon as the signal passes through the reactor containing the catalyst. As already discussed (*4*), curve M can be represented by the response of a mixed-flow reactor (CSTR) to the forcing function F.

For the curve labeled ^{13}CO(g), y represents the fraction of ^{13}CO in the gaseous CO at the reactor outlet. Thus if there were no adsorption or reaction of CO, ^{13}CO(g) and M would be identical. It is easy to show (*13*) by a material balance that the area of the difference between the actual ^{13}CO response of Fig. 1 and the mixing curve is proportional to the amount of CO adsorbed, assuming that all the surface ^{12}CO is replaced by ^{13}CO. From the mass of the catalyst, the CO conversion, the composition of the isotopic mixture (*13*), and the fraction exposed of the Rh obtained by H_2 adsorption (*1*), it is calculated that the surface coverage of CO is 0.87. Further experiments at 220°C give for times in ^{12}CO/H_2 of 600, 1800, and 3600 s, values of θ_{CO} of 0.65, 0.62, and 0.61.

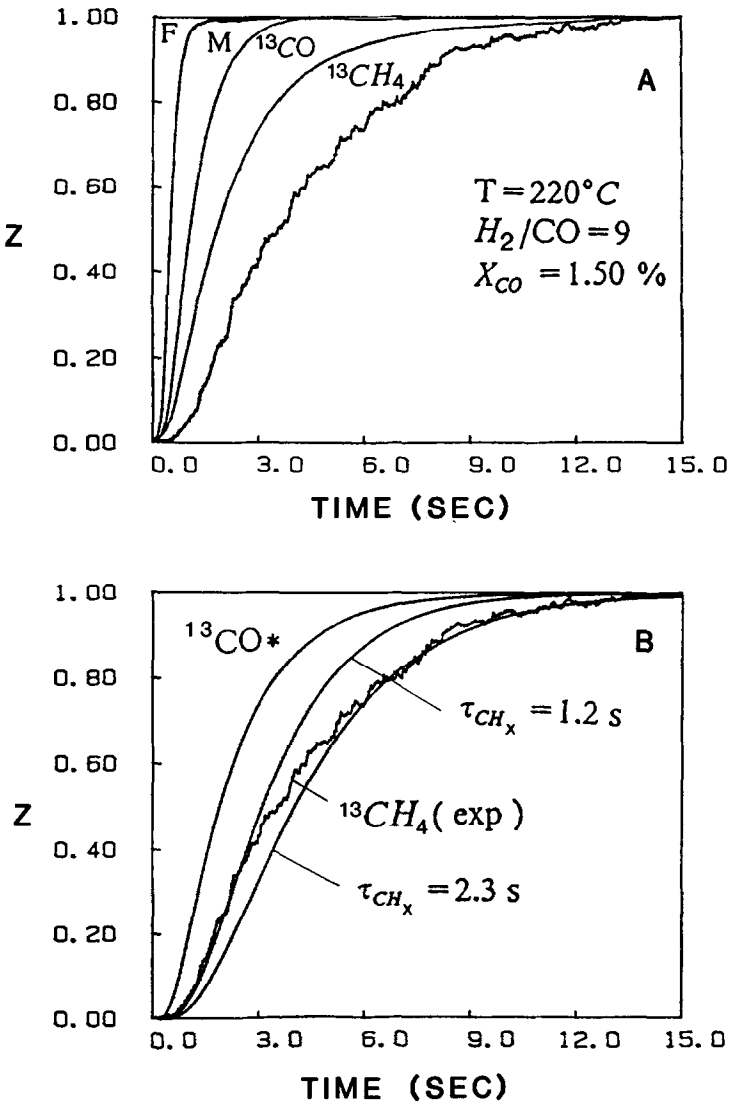

FIG. 1. (A) Experimental responses of forcing (F), mixing (M), gas phase ^{13}CO, and $^{13}CH_4$ obtained according to the delivery sequence: He(180 s) → $^{12}CO/H_2$(120 s) → $^{13}CO/H_2(t)$. T = 220°C, H_2/CO = 9. (B) Simulated responses of $^{13}CO*$ and $^{13}CH_4$ for the results of (A).

If the exchange between gaseous CO and adsorbed CO* is very fast, it is clear that Z(CO) and Z(CO*) should be identical. However, such may not be the case, and a parameter β can be defined as R_-/R_F, where R_- is the desorption rate of CO and R_F is the feed rate of CO (*4*). Fast exchange corresponds to $\beta \rightarrow \infty$, and irreversible adsorption of CO to $\beta \rightarrow 0$. Consideration of the pertinent differential equations, and simulations (*4*), leads to the realization that a relatively low desorption rate (say β = 0.5) means that the response of the surface $^{13}CO*$ is slower than that for the gas phase ^{13}CO(g).

The above considerations are important in the interpretation of the observed $^{13}CH_4$ response of Fig. 1A. It is assumed that the reaction sequence passes through CO* irreversibly to an adsorbed intermediate C_α,

which is irreversibly hydrogenated to CH_4. Thus the dynamics of the appearance of $^{13}CH_4$ is related to the rate of change of $^{12}CO^*$ to $^{13}CO^*$ (the forcing function for this step) and to the amount of intermediate for which the carbon content must change from ^{12}C to ^{13}C. The analytical equations representing this process have been developed (*4, 13, 5*). In order to obtain the best fit to the $^{13}CO(g)$ curve of Fig. 1A it has been found that β should be 2.2. This value, together with the other experimental conditions used, gives a mean lifetime τ_{CO^*} for the surface CO molecule of 35 ms. The Z for $^{13}CO^*$ can be calculated, as shown in Fig. 1B. Using this forcing function, the experimental Z for $^{13}CH_4$ can be modeled, where

$$\tau_{CH_x} = \theta_{CH_x}/TOF_{CH_x}. \qquad (2)$$

Here τ_{CH_x} is the response time of the pool of CH_x intermediate through which carbon is passing at a turnover rate for the total production of hydrocarbons (TOF_{CH_x}) of 1.7×10^{-2} s^{-1} for the conditions at hand. Thus the two values for τ_{CH_x} shown in Fig. 1B lead to $\theta_{C_\alpha} = 0.02$ or $\theta_{C_\alpha} = 0.039$. From Part I (*1*) it was found by the quenching/TPR procedure that $\theta_{C_\alpha} = 0.040$. For 10 min, 30 min, and 1 h in $^{12}CO/H_2$, similar $^{13}CH_4$ results were obtained, all very close to each other. This result indicates that the coverage of C_α remains about the same, as was found by the quenching/TPR experiment.

The active intermediate certainly seems to be the C_α mentioned above (*1*). The lack of fit of the simple model based on one τ to the experimental curve for $^{13}CH_4$ probably means that the C_α is of nonuniform reactivity, as has been noted previously (*4, 5, 16*) for other surface carbons.

Experimental steady-state tracing results at 260°C are presented in Fig. 2A for 2 min and 1 h on stream in $^{12}CO/H_2$. At this temperature the values of θ_{CO} found are 0.68, 0.52, 0.53, and 0.49 after 2 min, 10 min, 30 min, and 1 h on stream.

Unlike the situation at other temperatures, it was not possible to find a value of β which reproduced well the $^{13}CO(g)$ curve, as shown in Fig. 2B for 1 h on stream. However, with $\beta = 0.75$ it is possible to obtain a Z curve for $^{13}CO^*$ which lies below the experimental Z for $^{13}CO(g)$. Then a good fit can be found for the $^{13}CH_4$ experimental curve, with $\tau_{C_\alpha} = 1.3$ s leading to $\theta_{C_\alpha} = 0.054$ for $TOF_{CH_x} = 4.2 \times 10^{-2}$ s^{-1}. This value agrees with that of 0.034 obtained from the quenching/TPR experiment (*1*).

Catalyst surface composition. Figure 3 shows the surface coverages obtained at 220 and 260°C as a function of time on stream in CO/H_2. The quantities have been obtained as follows:

1. θ_{CO} is determined by the steady-state tracing experiment.

2. θ_{C_α} is obtained from the quenching/TPR experiment described in Part I (*1*). Although some CO may desorb after the switch to He and cooling to 100°C, the C_α on the surface is probably not affected. In addition the coverage of C_α so obtained is in quantitative agreement with that from the steady-state tracing results. The latter provide strong evidence that C_α represents the active intermediate from which methane is produced.

3. θ_{CS} is obtained by the direct switch from CO/H_2 to H_2 (*1*). After the switch to hydrogen, the decay of the CO signal has been followed in order to measure the amount of CO isothermally desorbed. This quantity is derived from the observed CO curve and the corresponding mixing curve. The latter refers to the CO decay that would be seen if there were no CO desorbed, so that the Z_{CO} curve would follow that of an argon tracer as it is washed out of the gas phase. The results of an example of such an experiment are presented in Table 1, where the first column is for CO desorption after a switch to H_2, and the second after a switch to He.

Table 1 shows that the desorption of CO under H_2 is quite small. For example, at 120 s and 220°C, Table 2 of Part I (*1*) shows $\theta_{CS} = 1.82$. This figure should be corrected

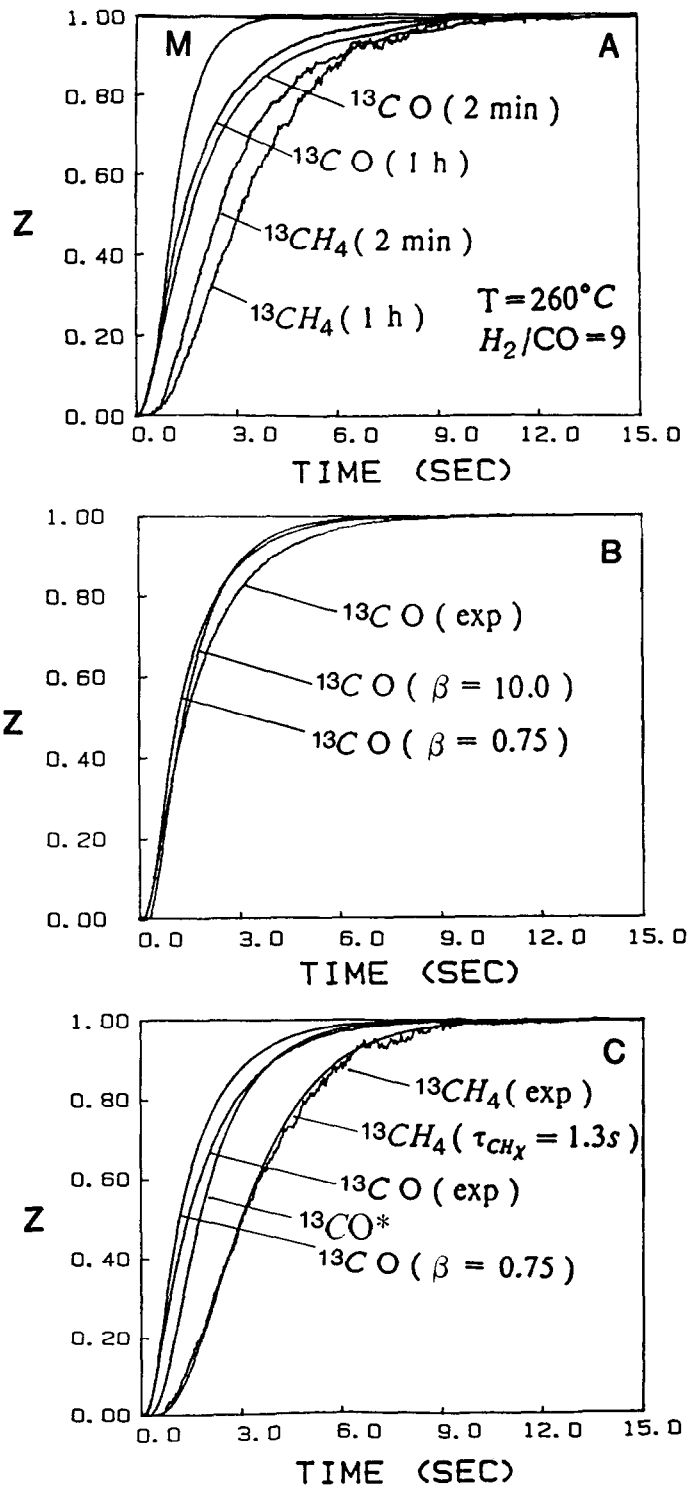

FIG. 2. (A) Experimental responses of mixing (M), gas phase ^{13}CO, and $^{13}CH_4$ obtained according to the delivery sequence: He(180 s) → $^{12}CO/H_2$(120 s) → $^{13}CO/H_2(t)$. T = 260°C, H_2/CO = 9. Also shown are the ^{13}CO(g) and the $^{13}CH_4$ responses after 1 h in $^{12}CO/H_2$. (B) Simulations and experiment for the ^{13}CO(g) response at 260°C, 1 h on stream. (C) Experimental curves at 260°C, 1 h on stream with the best simulation to be found (β = 0.75).

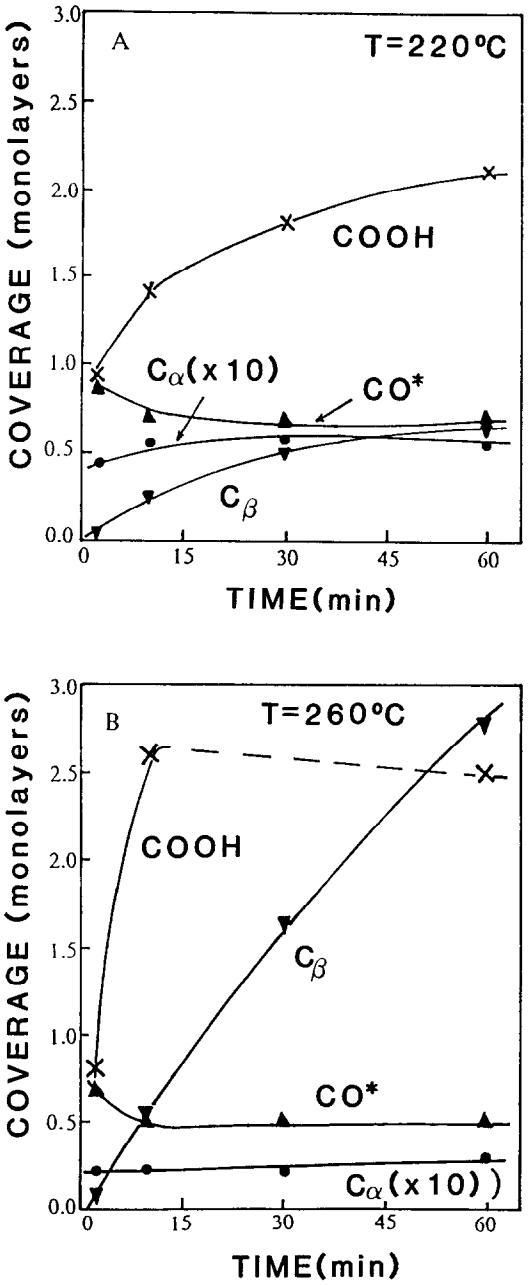

FIG. 3. (A) Time dependence of surface coverage of species present during synthesis at 220°C and $H_2/CO = 9$. (B) Time dependence of surface coverage of species present during synthesis at 260°C and $H_2/CO = 9$. Coverage values are based on 60 μmol Rh_s/g cat and a 30-mg sample.

by adding 0.064 from Table 1. These corrections are incorporated into the calculations leading to Fig. 3. θ_{CS} is not shown in Fig. 3 but is used to calculate θ_{COOH}.

From Table 1 it is clear that quite a bit of CO is lost in the helium treatment preceding the quenching/TPR experiment. However, these TPR were used only to calculate the coverages of C_α and C_β.

After the switch to H_2 and the isothermal hydrogenation, the temperature is programed to 450°C as shown in Part I (*1*) in order to remove the more refractory carbonaceous species. This carbon is included in θ_{CS}.

4. θ_{C_β} is obtained either from the isothermal plus TPR experiment of condition 3 above or from the quenching/TPR experiment of condition 2 above. C_β is defined as equivalent to the methane produced above 350°C in the TPR.

5. Finally, θ_{COOH} is derived from the relation

$$\theta_{COOH} = \theta_{CS} - \theta_{CO} - \theta_{C_\alpha} - \theta_{C_\beta}. \quad (3)$$

The surface composition at 180°C was previously given (*14*). We now describe some experiments aimed at verifying the correctness of Eq. (3) for the calculation of θ_{COOH}.

Isotopic characterization of the formate. In Fig. 4 are represented some experiments at 180°C, where the formation of C_β can be neglected at the short times shown (*14*). Figure 4A shows the result of a switch to hydrogen after 2 and 10 min on stream in

TABLE 1

Isothermal CO Desorption after 120 s in He or H_2 Stream. Delivery Sequence: CO/H_2 (120 s) → $H_2(t)$ or He(t)

T (°C)	CO desorption (monolayers) after 120 s	
	In H_2 stream[a]	In He stream[b]
180	0.095	0.040
200	—[c]	0.100
220	0.064	0.160
240	—[c]	0.210
260	0.036	0.320

[a] After 120 s in H_2, no further CO is desorbed.
[b] After 120 s in He, desorption of CO is still occurring.
[c] Not measured.

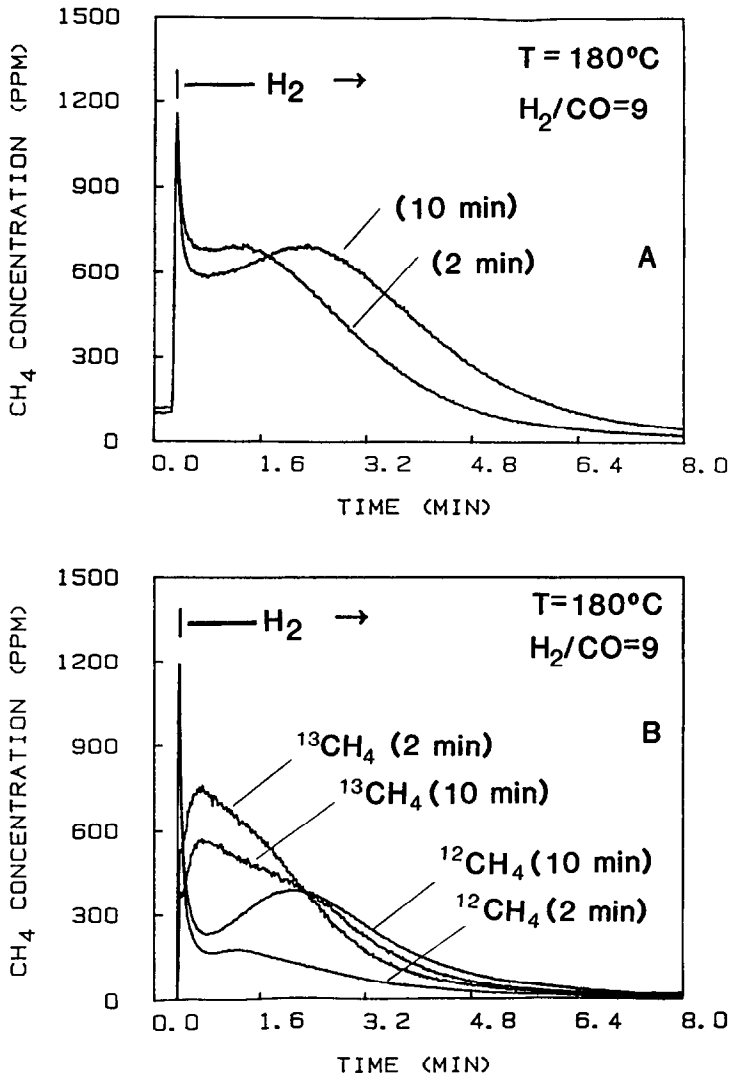

FIG. 4. (A) Transient response of CH_4 under the sequence: He(180 s) → $CO/H_2(\Delta t)$ → $H_2(t)$ at 180°C. (B) Isotopic transient experiment for deconvoluting the CH_4 response obtained in (A) according to the delivery sequence: He(180 s) → $CO/H_2(\Delta t)$ → ^{13}CO/He(40 s) → $H_2(t)$.

H_2/CO, leading to the isothermal titration of all the surface carbonaceous species. The initial sharp peak represents C_α and it can be nicely separated from the following broad peaks by the quenching/TPR (*1*, *14*).

Figure 4B shows an isotopic deconvolution in which the reaction is quenched by a switch from $^{12}CO/H_2$ to ^{13}CO/He before the isothermal hydrogen titration. During the exposure to ^{13}CO/He (40 s), methane production stops, and the $^{12}C_\alpha$ is not replaced by new $^{13}C_\alpha$. Also, negligible new $^{13}C_\alpha$ is produced by ^{13}CO disproportionation, since there is almost no $^{13}CO_2$ production. However, the adsorbed ^{12}CO exchanges rapidly with the ^{13}CO in the gas phase. Thus in Fig. 4B the $^{13}CH_4$ peak arises from adsorbed CO, and the $^{12}CH_4$ peaks arise from C_α and COOH. The results are summarized in Table 2. The coverage of CO remains about unity, in agreement with the steady-state tracing results and also with the simple ad-

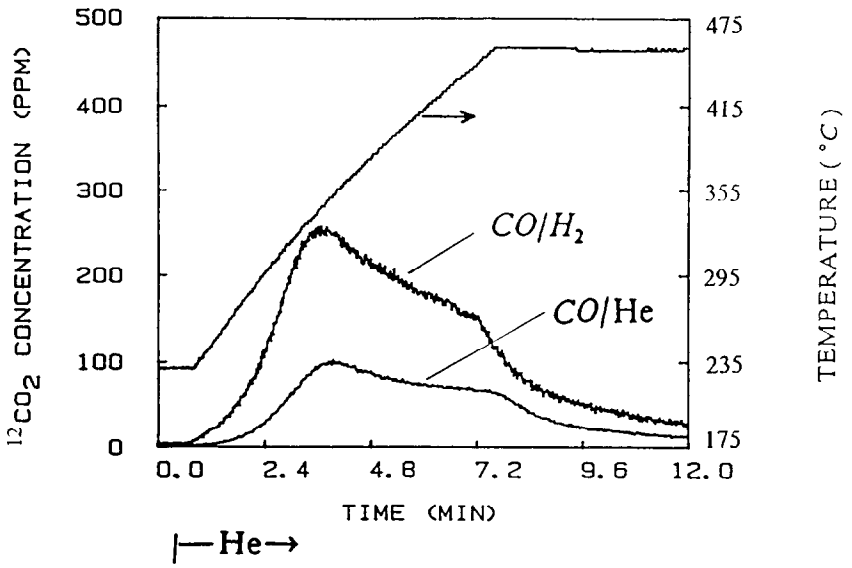

FIG. 5. $^{12}CO_2$ production under the following delivery sequence: He(180 s) → CO/H_2(600 s) or CO/He(600 s), 220°C → ^{13}CO/He(40 s), 220°C → He(t), TPR.

sorption of CO at 180°C (*14*). The values of θ_{COOH} from Eq. (3) are in satisfactory agreement with those from Fig. 4B. The results of Fig. 4B have been repeated with times of exposure to ^{13}CO/He of up to 5 min. A subsequent switch to H_2 produces $^{12}CH_4$ and $^{13}CH_4$ curves very close to those of Fig. 4B, obtained after 40 s in ^{13}CO/He.

It is clear that all the results so far agree with the premise that the formate species does not participate in the reaction sequence and does not exchange with gaseous CO. As argued from the infrared results, the formate resides on the alumina.

Another isotopic experiment is shown in Fig. 5. After 10 min in $^{12}CO/H_2$ at 220°C, the surface ^{12}CO was exchanged with gaseous ^{13}CO, as in Fig. 4B. However, instead of a switch to H_2, in Fig. 5 the switch is to He, with an immediate ramping of the temperature to give a temperature programed reaction on the surface, producing mostly CO_2 and H_2. We are not interested in the tagged species, which arise from the surface CO. The area under the upper curve corresponds to θ_{COOH} = 0.92, to be compared to 1.35 from Fig. 3A, based on hydrogen titration and Eq. (3). As shown by Solymosi *et al.* (*6*), exposure of the formate on Rh/Al_2O_3 to He up to high temperatures was not sufficient to remove all the COOH bands. Complete removal requires reaction in H_2.

TABLE 2

Determination of Formate at 180°C

Time in $^{12}CO/H_2$ (min)	θ_{CS} (Fig. 4A)	θ_{CO} (Fig. 4B)	θ_{COOH} (Fig. 4B)	θ_{CS} (Fig. 4B)	θ_{COOH} (Eq. (3))
2	1.61	1.10	0.50	1.60	0.59
10	2.17	1.06	1.00	2.06	1.00

The lower curve in Fig. 5 arises from the decomposition of adsorbed formate generated in the absence of hydrogen. The area under the curve corresponds to θ_{COOH} = 0.30. Although the generation of formate from CO is favored by the presence of H_2 (*1*), Gopal *et al.* (*11*) have found that formate can appear on Al_2O_3 alone in the presence of CO alone. Our results indicate that part of the formate made in the absence of H_2 seems to be relatively unreactive to hydrogen titration.

In view of the above results, it is of interest to study the interaction of CO with a

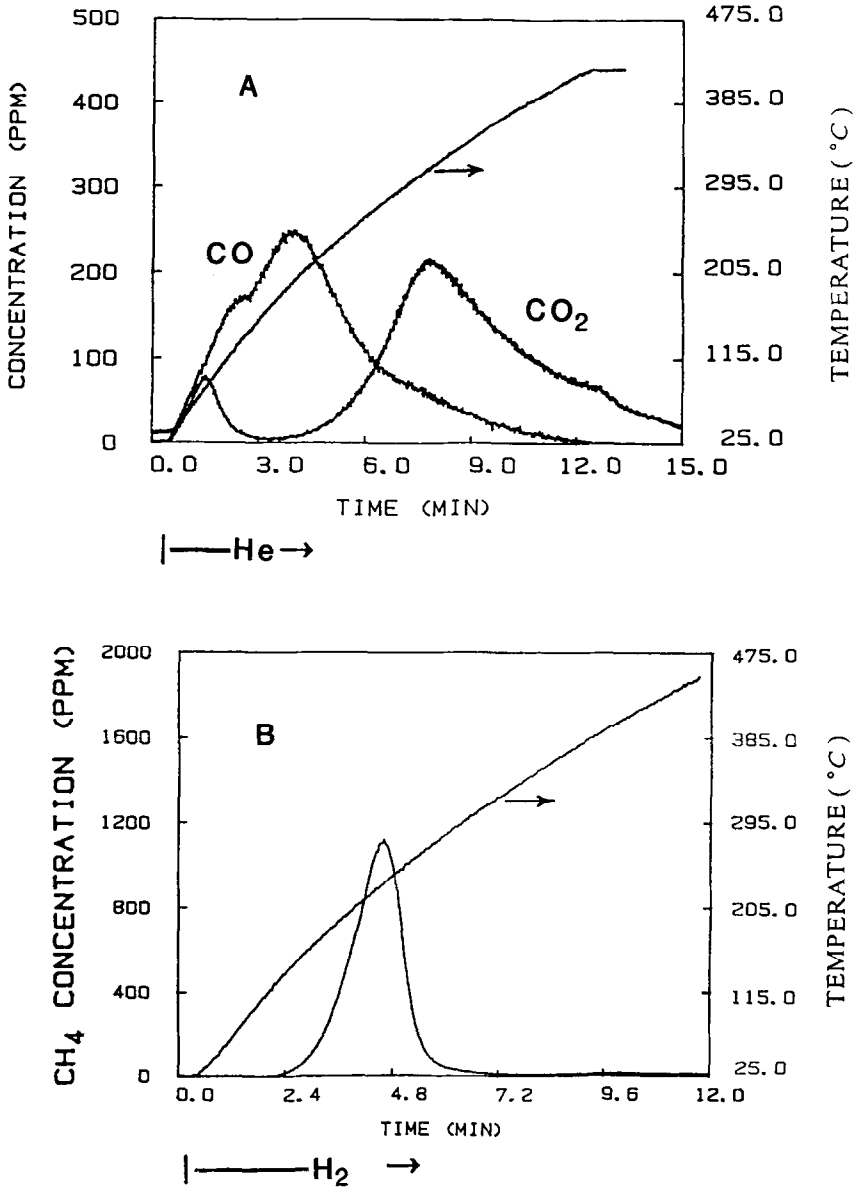

FIG. 6. (A) Temperature programed desorption of CO and CO_2 on a used sample, after the delivery sequence: CO/He(1200 s), 40°C → He(60 s), 40°C → He(t), TPD. (B) Hydrogenation of CO under the delivery sequence: CO/He(1200 s), 28°C → He(60 s), 28°C → H_2(t), TPR.

used catalyst at near room temperature. Figure 6A shows that a TPD produces both CO and CO_2, and the total quantities correspond to $\theta_{CO} = 1.24$, neglecting any contribution of the Boudouard reaction on the surface. Figure 6B shows that a TPR instead of a TPD produces a tall narrow peak of CH_4 at 235°C corresponding to $\theta_{CO} = 1.10$. The added CO and CO_2 desorbed during the TPR add another 0.1 monolayer, bringing the CO adsorbed as measured by Figs. 6A and B into agreement. Clearly there is a small amount of formate on the surface during these experiments. The

results agree with those of Fujimoto *et al.* (*17*).

Blank experiments. The reactor was loaded with the same amount of alumina alone as was used in the work with the 5% Rh/Al_2O_3, and a number of experiments were performed. In the range of temperatures 180–240°C, passing CO/H_2 through the reactor produced no products, but at 260°C the result shown in Fig. 7 was obtained for 1 h on stream. The reaction rate is about 1.7% of that found over 5% Rh/Al_2O_3 for the same conditions. A switch to H_2 followed by a TPR produces a quantity of methane equivalent to $\theta_{CS} = 0.8$, referred to the supported rhodium catalyst, in 12 min as shown. The amount of inactive carbon C_β is 0.65 monolayer. Probably this methane comes from the slow hydrogenation of formate on the support, as suggested by Gopal *et al.* (*11*). From Fig. 3 the amount of formate on the Rh/Al_2O_3 catalyst for the same conditions corresponds to $\theta = 2.5$.

Steady-state tracing experiments at 180, 220, and 260°C on alumina alone after 120 s of passage of $^{12}CO/H_2$ show no exchange of ^{13}CO with the surface. In other words, after the switch from $^{12}CO/H_2$ to $^{13}CO/H_2$, the $Z(^{13}CO)$ curve rises on top of the mixing curve. Any formate on the alumina does not exchange with gaseous CO.

There is no measurable adsorption of CO on Al_2O_3 at room temperature, in contrast to the result of Fig. 6A. The experiment of Fig. 5 gave no CO_2 production with alumina alone, consistent with the results of Gopal *et al.* (*11*).

Response to a helium purge. After 120 s of reaction time in CO/He at 220°C, a switch to He has been made, followed by H_2 titration. Since the formate generated is small in quantity and decomposes very slowly in the absence of a temperature ramp, the gas desorbed during the He purge is CO. Typical results are shown in Fig. 8, and the data obtained are summarized in Fig. 9. It is interesting to compare the results for θ_{CS} with no purge to those after 120 s of He. The amounts of CO desorbed in 120 s can then be calculated as 0.09 at 180°C, 0.18 at 220°C, and 0.32 at 260°C. Reference to Table 1 shows good agreement with the amounts derived from the di-

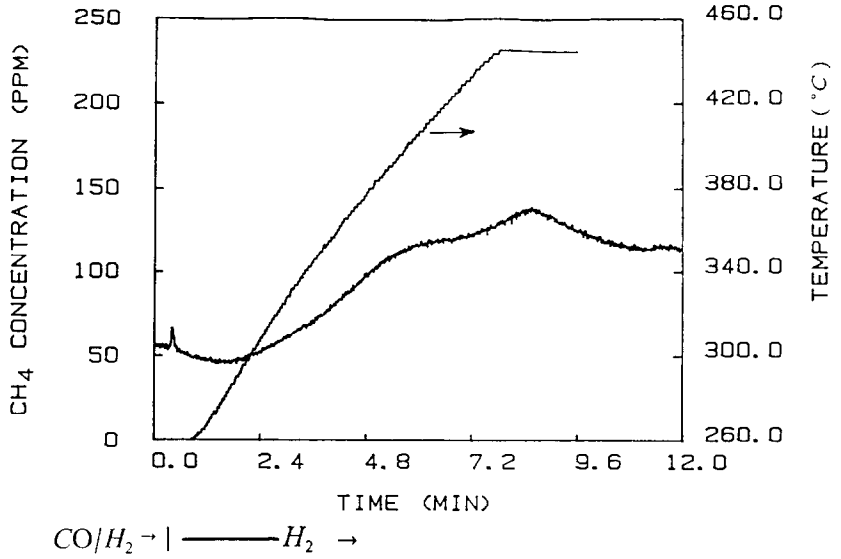

FIG. 7. Activity of Al_2O_3 alone. Delivery sequence: H_2(4 h), 350°C → 260°C → He(180 s), 260°C → CO/H_2(1 h), 260°C → $H_2(t)$, TPR.

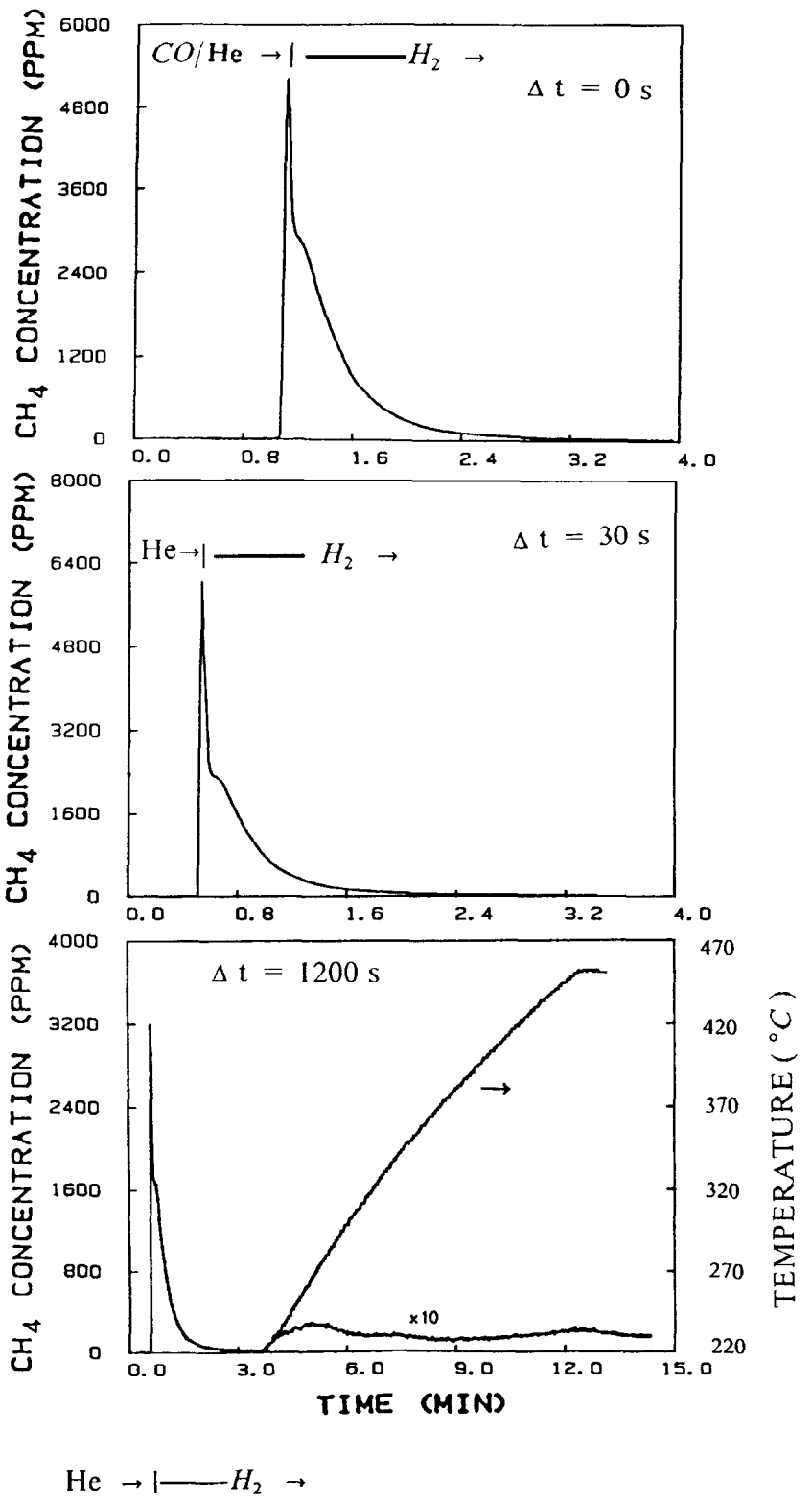

FIG. 8. Transient response of CH_4 under the sequence: He(180 s) → CO/He(120 s) → He(Δt) → $H_2(t)$, at 220°C and He/CO = 9. For Δt = 1200 s, after the isothermal H_2 reduction T is increased as shown.

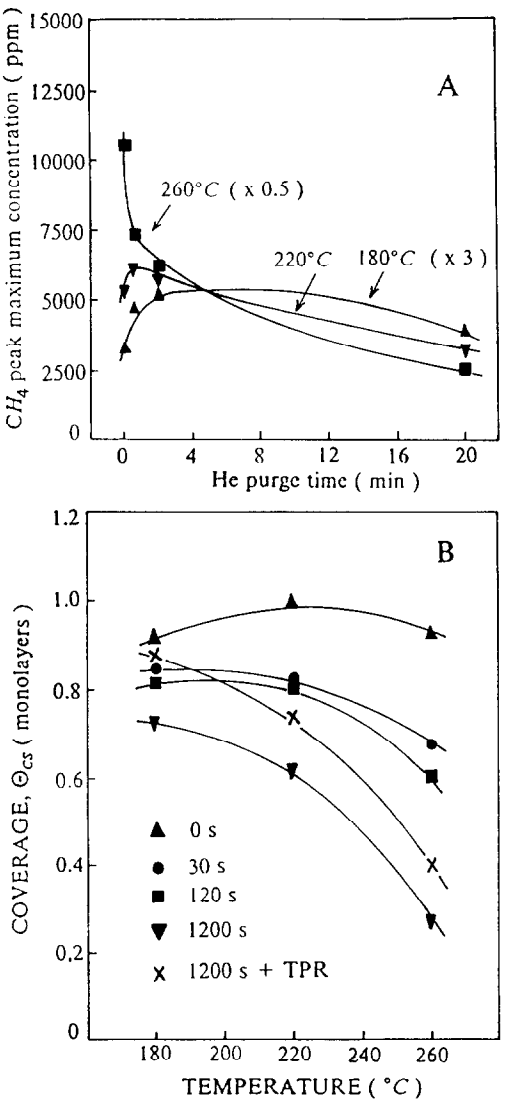

FIG. 9. (A) CH_4 peak maximum concentration appearing at the switch to H_2 vs He purge time. Delivery sequence: He(180 s) → CO/He(120 s) → He(Δt) → $H_2(t)$. (B) Coverage of carbonaceous species vs temperature for various He purge times. The coverage of carbonaceous species corresponds to the equivalent CH_4 obtained by isothermal H_2 titration. Delivery sequence: He(180 s) → CO/He(120 s) → He(Δt) → $H_2(t)$.

rect measurement of the CO desorption, taking into account the effect of adsorbed hydrogen on the CO desorption.

A similar experiment is shown in Fig. 10, where the He purge follows 2 min of the CO/H_2 reaction. Now much formate is made, so the curves of Fig. 11 show much larger decreases in θ_{CS} than those of Fig. 9, as both CO and CO_2 (ex COOH) desorb. A small peak of CH_4 is also observed during the He purge at various temperatures, in agreement with Solymosi *et al.* (*6*).

The behavior of C_α and C_β. Figure 12 shows how at 220°C the coverage of active carbon C_α and inactive carbon C_β vary with time in three different circumstances. In both cases, Figs. 12A and B, the amounts of C_α and C_β were obtained by the quenching/TPR procedure (*1*).

From Fig. 12A it is seen that the amount of C_α is about the same, whether it is produced by the CO/H_2 reaction or by the interaction of CO/He with the catalyst. This result will be discussed later, since it is often found that hydrogen promotes the dissociation of CO. The figure also shows that a 15-min purge in He partially deactivates the C_α. Of course, since coverage of C_α is so small, it is not possible to measure the corresponding increase in the coverage of C_β.

Figure 12B shows how C_β behaves in the same experiments as described above. Here it is interesting to note that the formation of C_β is enhanced by the presence of hydrogen. However, exposure of C_β to He for 15 min does not have much effect on its reactivity.

More results at 260°C. In the quenching/TPR results given in Part I (*1*), after reaction in CO/H_2 for 2 min, the COOH peak was confounded with the CO peak, and the C_β appeared as a tail or a very flat peak above 350°C. However, for longer times on stream at 260°C, the results of Fig. 13 are obtained.

Figure 13B for 600 s in CO/He shows a result like those given before (*1*), with a sharp peak for C_α, a large peak for CO, and a long tail for inactive formate and C_β. For the same time in CO/H_2, Fig. 13A indicates, as usual, a larger principal peak (CO + COOH), but now there is a new peak at 300°C. For longer times on stream this peak moves to higher temperatures: 340°C at

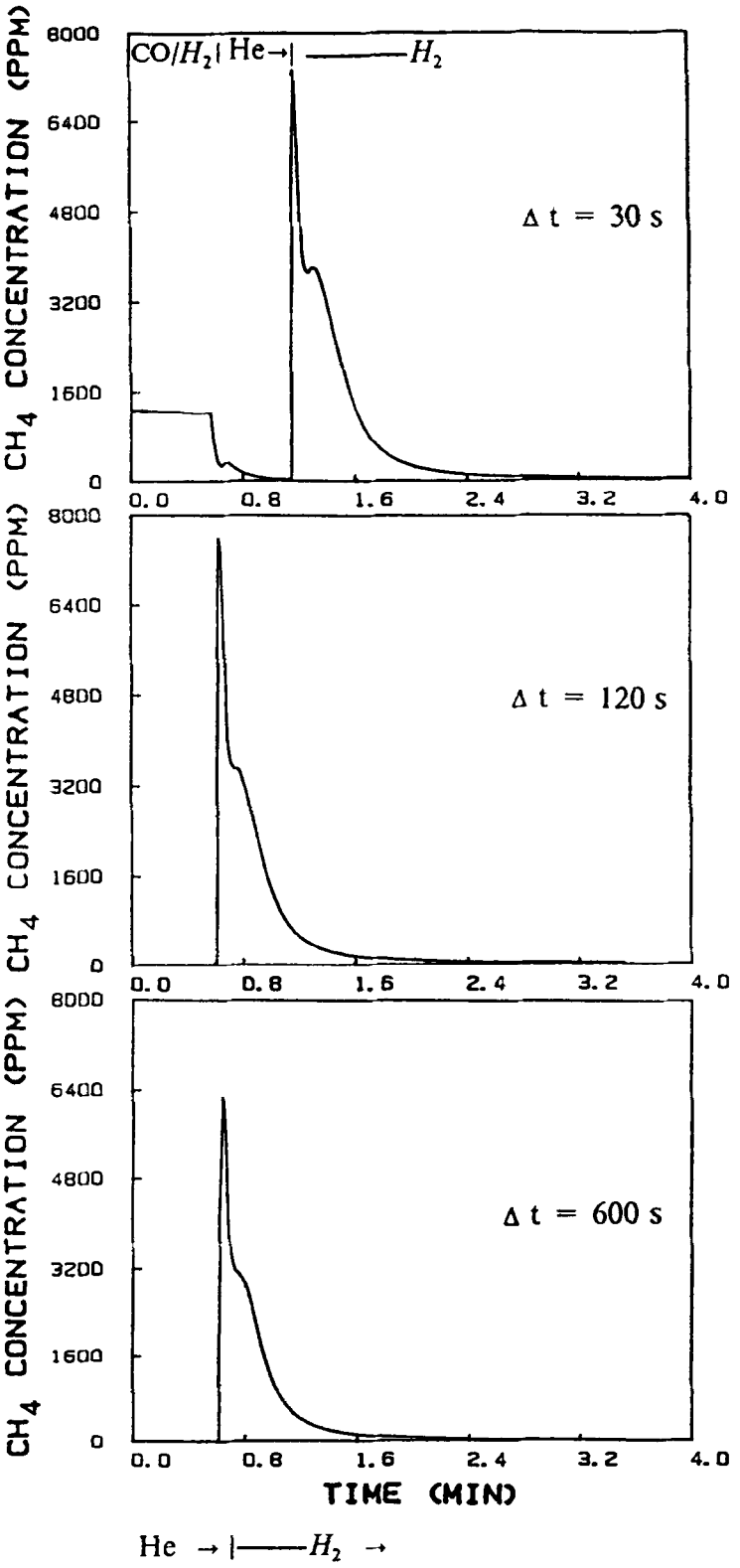

FIG. 10. Transient response of CH_4 under the sequence: He(180 s) → CO/H_2(120 s) → He(Δt) → $H_2(t)$, at 220°C and $H_2/CO = 9$.

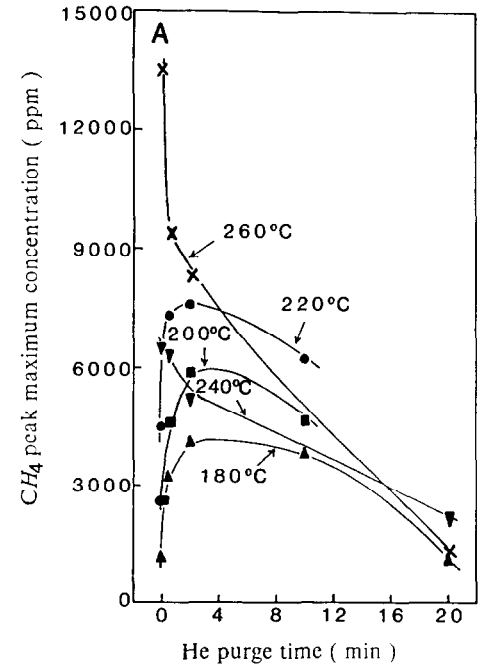

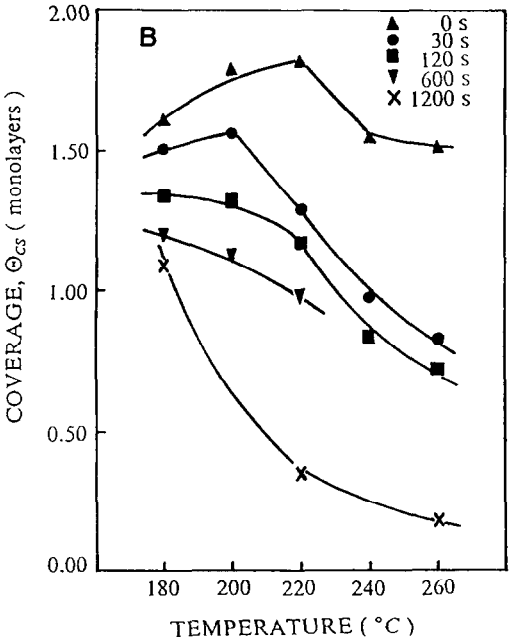

FIG. 11. (A) CH_4 peak maximum concentration appearing at the switch to H_2 vs He purge time. Delivery sequence: He(180 s) → CO/H_2(120 s) → He(Δt) → $H_2(t)$. (B) Coverage of carbonaceous species vs temperature for various He purge times. The coverage of carbonaceous species corresponds to the equivalent CH_4 obtained after isothermal H_2 titration. Delivery sequence: He(180 s) → CO/H_2(120 s) → He(Δt) → $H_2(t)$.

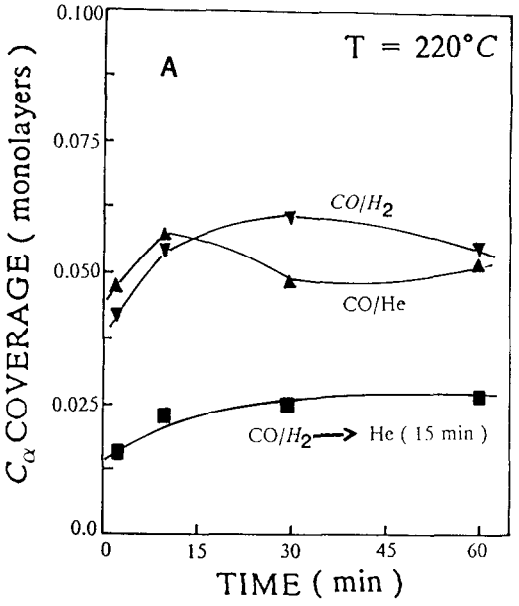

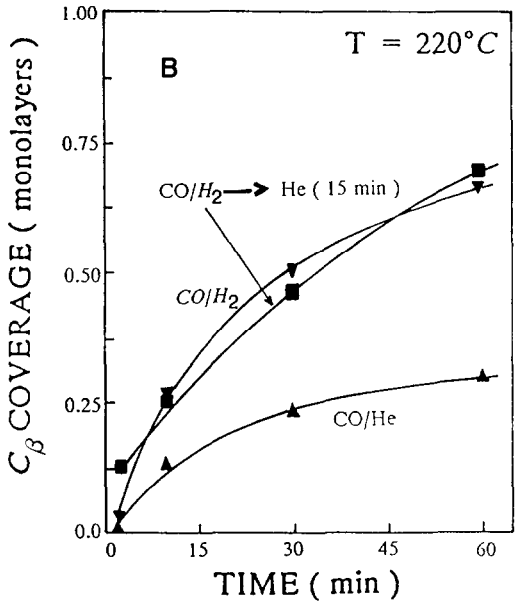

FIG. 12. (A) Time dependence of surface coverage of active C_α species as obtained from three different TPR deconvolution experiments: (1) He(180 s) → $CO/H_2(\Delta t)$, 220°C → He, cool-down to 100°C → $H_2(t)$, TPR. (2) He(180 s) → $CO/H_2(\Delta t)$, 220°C → He(15 min at 220°C) → cool-down in He to 100°C → $H_2(t)$, TPR. (3) He(180 s) → CO/He(Δt), 220°C → He, cool-down to 100°C → $H_2(t)$, TPR. (B) Time dependence of surface coverage of inactive C_β species as obtained under the conditions described in (A).

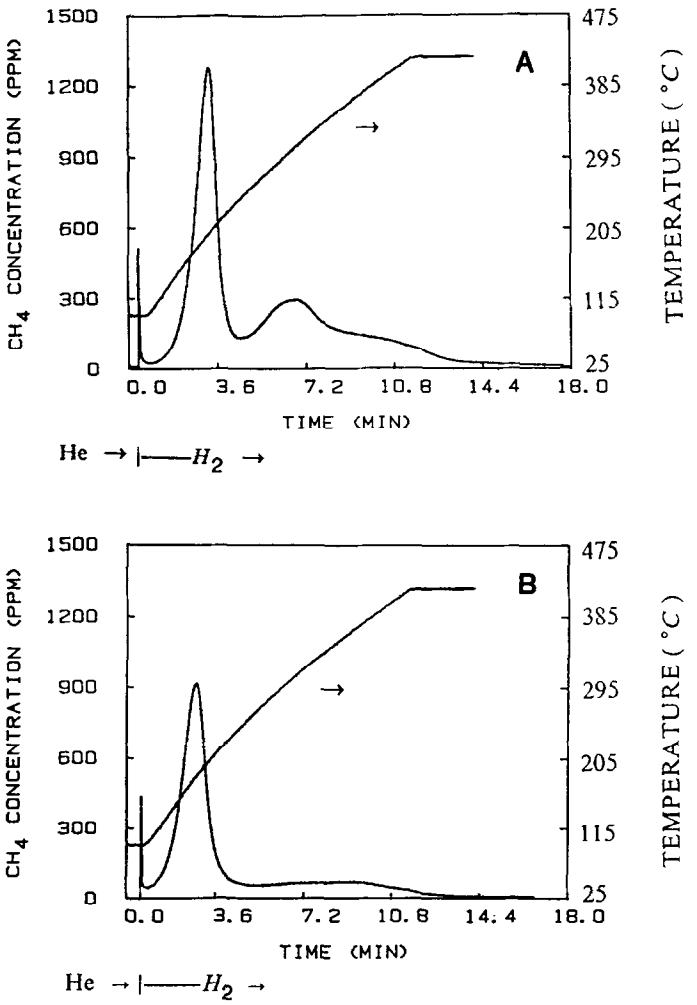

FIG. 13. (A) TPR deconvolution experiment according to the delivery sequence: He(180 s) → CO/H_2(600 s), 260°C → He, cool-down to 100°C → $H_2(t)$, TPR. (B) TPR deconvolution experiment according to the delivery sequence: He(180 s) → CO/He(600 s), 260°C → He, cool-down to 100°C → $H_2(t)$, TPR.

1800 s and 350°C at 3600 s. The shoulder at about 385°C, attributed to C_β, grows with time on stream without changing temperature. The peak which has a maximum in the range 300–350°C seems to be a new species, but its nature has not been further investigated in this work. In Fig. 3B some of the carbon attributed to C_β may be formate or yet a different species of carbon. The same is true for the estimated amount of formate, where some other species of carbon might be reacted away at $T < 350$°C, thus giving an overestimate for the amount of formate.

DISCUSSION

Steady-state tracing. The estimate of the amount of CH_x intermediate can in principle be made from the $^{12}CH_4$ decay curve after the switch from $^{12}CO/H_2$ to $^{13}CO/H_2$ if it can be assumed that the exchange rate is fast compared to the reaction rate. For this fast exchange, the fraction of ^{13}C in the CO* pool on the surface is essentially the

same as that in the CO(g), during the transient. Such is the case for Fig. 1 ($\beta = 2.2$), and for similar experiments on Ni/Al_2O_3 (*4*). In the present study, the value of β is smaller, making necessary a mathematical simulation of the process in order to obtain correctly the amount of the CH_x intermediate. This procedure is particularly important for the present experiments, because the ^{13}CO response and the $^{13}CH_4$ response are so close together. The lack of close fit for the $^{13}CH_4$ response in Fig. 1B can be attributed to a nonuniform reactivity of the active surface carbon C_α.

If the CO exchange is not relatively rapid, then the $^{13}CO^*$ response lags behind the ^{13}CO response in the gas phase, as shown for these curves in Fig. 2C, where the simulation is based on $\beta = 0.75$. However, it has not been possible to fit the CO(exp) curve by the calculated CO curve, with $\beta = 0.75$ or any other value. With $\beta = 0.75$ and $\tau_{CH_x} = 1.3$ s, there is a good fit between the simulated and the experimental curves for $^{13}CH_4$. This anomalous situation is probably connected with the results of Figs. 3 and 13. At 260°C the surface coverage of C_β is high and quite different from those found in the range 180–240°C. Thus the mathematical model used may not be suitable to represent these experiments. Dalla Betta and Shelef (*9*), for a Ru/Al_2O_3 catalyst, found that at temperatures higher than 250°C, the metal surface is altered, possibly by the presence of carbon. Then adsorbed CO exhibits a lower stretching frequency and a reduced intensity.

Although these difficulties detract from the precision of the estimate of C_α from the tracing experiments, it is clear that the pool of active species through which carbon passes to make methane usually amounts to less than 5% of a monolayer of rhodium. The quenching/TPR studies (*1*) indicate a similar coverage of C_α and so reinforce the isotopic results.

The CO coverage calculated from the tracing results depends on the assumption that the CO group in the COOH does not exchange with gaseous or surface CO. This assumption is supported by the following observations.

1. For low temperatures, θ_{CO} from the quenching/TPR experiment after CO/He (*1*) is about the same as that obtained from the steady-state tracing studies.

2. The isotopic experiments of Fig. 4 and Table 2 lead to values of θ_{CO} and θ_{COOH} which agree with those of Fig. 3, in which θ_{COOH} was based on Eq. (3). In this equation, θ_{CO} was obtained from the steady-state tracing experiments.

The results of the present study show that there is no exchange of CO with the carbonyl of COOH. However, Solymosi *et al.* (*7*) found that D_2 can readily exchange with the H of the formate. This process probably occurs by spillover with dissociation on the metal. This route is not available to CO.

Isotopic experiments like those of Fig. 4 have been used (*4*) to calculate the amount of CH_x intermediate from the $^{12}CH_4$ response and the surface CO coverage from the $^{13}CH_4$ response. This procedure is valid only if no other surface species react with H_2 to give methane. For Rh/Al_2O_3, the reaction of formate with H_2 greatly contributes to the $^{12}CH_4$ response, so that the coverage of CH_x cannot be obtained from this experiment. The He quenching/TPR experiment (Part I (*1*)) and the steady-state tracing (Figs. 1 and 2) provide alternative routes for measuring CH_x.

Distinction between COOH and C_β. Since on Fe/Al_2O_3 (*5*) and Ru/SiO_2 (*18, 19*) the nonexchangeable surface carbon is all reported as CH_x, it is important to show evidence that for Rh/Al_2O_3 much of this surface carbon is incorporated in the formate species. It is recalled that Solymosi *et al.* (*7*) found that the infrared bands for formate were stable at 250°C but removable by hydrogen. However, above this temperature the formate under helium is decomposed to form CO_2 and H_2. For Rh/Al_2O_3, very little CO is formed. Thus the results of

Fig. 5, which show that $^{12}CO_2$ is formed from the nonexchanged surface carbonaceous species, are important. The C_β is not expected to produce CO_2 under a helium TPD. Then the $^{12}CH_4$ response of Fig. 4B logically arises from C_α followed by COOH. As discussed elsewhere, the C_β is taken as represented by the CH_4 which appears in a TPR above 350°C.

Figures 4 and 5 demonstrate that the growing and shifting of the second peak in Fig. 4 (peak 3, Part I (*1*)) is caused by the growth of the formate species. Zhou and Gulari (*25*) obtained a result like that of Fig. 4A for their Ru/Al_2O_3 catalyst. However, these authors assign the peak to an active CH_x intermediate. They do not mention the possibility of the existence of formate, despite the results of Dalla Betta and Shelef (*9*).

The rapid growth and subsequent saturation of the formate coverage shown in Fig. 3 is a behavior which is similar to that shown by the formate bands in Fig. 7 of Ref. (*7*).

Relation between surface coverage and kinetics. The ideal way to understand the kinetics of the reaction system would be to develop a complete mathematical model which would predict the surface and gas phase compositions as a function of time and temperature. This procedure has been possible for a simple system, N_2O decomposition (*20*), and for a complex system, CO oxidation (*21, 22*). We hope to use the data of the present study for such an enterprise, but for the moment let us consider some qualitative features of the kinetics.

Since the surface coverage of CO is relatively high and that of C_α relatively low, the rate of methane production is mostly controlled by the dissociation of CO*. However, "complete" control by this step would mean that the response of $^{13}CH_4$ of Fig. 1A would be essentially superposed on that of ^{13}CO, assuming rapid exchange so that $Z_{CO} = Z_{CO^*}$. Then θ_{C_α} would be immeasurably small, but such is not the case. Perhaps the existence of a single rate-determining step with other steps in pseudo-equilibrium is not a process as common as has often been assumed (*23*). Recall that in the study of the CO/H_2 reaction over Fe/Al_2O_3 (*5*) it was found that the opposite situation prevailed. There is a relatively small coverage of CO and a relatively large coverage of CH. However, θ_{CO} is not zero, but of the order of 10%, so that it can only be said that the hydrogenation of CH predominates in controlling the rate. For the CO/H_2 reaction over Ni/Al_2O_3, both coverages of CO and C_α are high, and there is clearly no rate-determining step (*4*).

It is to be noted in Fig. 3 that there is a slight decrease in θ_{CO} and a slight increase in θ_{C_α} with time. These changes coincide with a decrease in the methane TOF (*1*), as rate control shifts somewhat toward the hydrogenation of C_α. We may speculate that as C_β covers more of the metal, θ_H must also decrease, along with θ^* (vacant sites). These effects could slow down the reaction rate without any dramatic changes in the coverages of CO or C_α. It seems difficult to devise any direct method of measuring θ^*. As for θ_H, this measurement can be attempted by deuterium exchange, but there are so many possibilities of exchange with the support, with water, or with surface CH_x that this experiment has not been attempted.

From the steady-state tracing results, the enthalpy and entropy of adsorption of CO at the coverage at steady-state can be estimated. For these calculations it is assumed that surface CO is in pseudo-equilibrium with gaseous CO. Data for short times on stream are used so that there is little C_β present. These calculations give 21.5 kcal mol^{-1} for the enthalpy change of adsorption, and 34.9 cal mol^{-1} K^{-1} for the entropy change.

The role of inhibiting species such as CO can be appreciated from the results of Figs. 10 and 11. Figure 11A shows that a short purge in helium after reaction in CO/H_2 at 180–220°C leads to a dramatic increase in the initial rate of hydrogenation (peak

height of methane) of the remaining surface species, probably because θ^* has been increased by the desorption of some CO. Of course the amount of species finally hydrogenated is lowered by the amounts of CO desorbed and COOH decomposed, as shown in Fig. 11B. For long times, the C_α is probably deactivated by its heat treatment in helium. At 240 and 260°C the θ^* before any purge is higher, so that there is no increase in the hydrogenation rate after various times in helium. The rate of deactivation of C_α is higher at these temperatures. Long exposure to He at 260°C causes the desorption of most of the CO, and the decomposition to CO_2 of much COOH. Thus the isothermal hydrogenation at 260°C leads to little CH_4 production. Most surface carbon is left as C_β, which is removed only by a TPR.

The results for CO/He, followed by a He purge, shown in Figs. 8 and 9, are similar, but in the absence of H_2 only a little, relatively inactive, COOH forms, so that the total carbonaceous surface coverages remain below 1.0. Less C_β is formed under He also, as shown in Fig. 12B. Perhaps this indicates that C_β may consist of somewhat hydrogenated carbon. Such a species exists on iron (*5*).

Species on the alumina. The alumina surface area (110 m^2/g), the Rh loading (5.2%), and the Rh fraction exposed (0.12) can be used to calculate that the ratio of exposed atoms of alumina to exposed Rh atoms is about 30. On this basis, the highest θ_{COOH} (2.5) amounts to amount 8.3% of the alumina surface. Supposedly the formate production can occur on the alumina over a large range of possible extents of hydroxylation. The generation of formate is markedly favored by the presence of hydrogen, which probably acts through dissociation on the Rh and spillover to the alumina (*7*). Formate generation in CO/He on Rh/Al_2O_3 or in CO/H_2 on Al_2O_3 is sharply limited (*7*). None was found by infrared measurements for CO/H_2 on Rh/SiO_2 (*6–8*).

Since the production of C_β is enhanced by the presence of H_2 with CO, and it forms to the extent of more than two monolayers of Rh, it is possible that some of this carbon is also present on the support.

It has already been mentioned that the CO/H_2 reaction rate increases in the order Rh/MgO, Rh/SiO_2, Rh/Al_2O_3, and Rh/TiO_2 (*7*). Since the formate on the alumina is a spectator species, it is difficult to link its presence to the increased activity of Rh/Al_2O_3 over Rh/SiO_2. In fact, formate is readily produced on Rh/MgO, a catalyst of *lower* activity than Rh/SiO_2. The metal particle sizes for the catalysts studied are not small enough to lead to important electronic effects via the interfaces between the metal particles and the support (*24*). A more probable explanation for the enhanced activity of Rh/Al_2O_3 is that for the alumina the interfacial perimeters between metal and support are increased by decoration of the metal by the support, and active sites may be associated with these perimeters. Clearly these active sites vary from one support to another depending on chemical properties such as the acidity and degree of hydroxylation. However, investigation of this notion would require studies by other spectroscopies, including techniques such as electron microscopy, Auger electron spectroscopy, or extended X-ray absorption fine structure spectroscopy, on the appropriate catalysts.

CONCLUSIONS

Transient isotopic methods confirm that the rate of the CO/H_2 reaction over 5% Rh/Al_2O_3 is largely controlled by the rate of dissociation of surface CO. However, there is also present on the rhodium a small pool of highly reactive surface carbon, through which the carbon from CO passes as it forms methane. The presence of formate has also been supported by the results, and this spectator species does not exchange with ^{13}CO nor participate in the methanation reaction.

Above 240°C, carbon generation on the catalyst is accelerated, and it appears that a

new species forms having a reactivity different from those observed at lower temperatures.

ACKNOWLEDGMENTS

Support of this work was provided by the National Science Foundation through Grant CBT-8517158 and by the University of Connecticut Research Foundation.

REFERENCES

1. Efstathiou, A. M., and Bennett, C. O., *J. Catal.* **120,** 118 (1989).
2. Happel, J., Suzuki, I., Kokayeff, P., and Fthenakis, V., *J. Catal.* **65,** 59 (1980).
3. Yang, C.-H., Soong, Y., and Biloen, P., *in* "Proceedings, 8th International Congress on Catalysis, Berlin, 1984," Vol. II, p. 3. Dechema, Frankfurt-am-Main, 1984.
4. Stockwell, D. M., Chung, J. S., and Bennett, C. O., *J. Catal.* **112,** 135 (1988).
5. Stockwell, D. M., Bianchi, D., and Bennett, C. O., *J. Catal.* **113,** 13 (1988).
6. Solymosi, F., Bansagi, T., and Erdöhelyi, A., *J. Catal.* **72,** 166 (1981).
7. Solymosi, F., Tombacz, I., and Kocsis, M., *J. Catal.* **75,** 78 (1982).
8. Erdöhelyi, A., and Solymosi, F., *J. Catal.* **84,** 446 (1983).
9. Dalla Betta, R. A., and Shelef, M., *J. Catal.* **48,** 111 (1977).
10. Amenomiya, Y., *J. Catal.* **57,** 64 (1979).
11. Gopal, P. G., Schneider, R. L., and Watters, K. L., *J. Catal.* **105,** 366 (1987).
12. Orita, H., Naito, S., and Tamaru, K., *J. Catal.* **111,** 464 (1988).
13. Efstathiou, A. M., Ph.D. thesis, University of Connecticut, 1989.
14. Efstathiou, A. M., and Bennett, C. O., *Chem. Eng. Commun.* **83,** 129 (1989).
15. Stockwell, D. M., and Bennett, C. O., *J. Catal.* **114,** 354 (1988).
16. De Pontes, M., Yakomizo, G. H., and Bell, A. T., *J. Catal.* **104,** 147 (1987).
17. Fujimoto, K., Kameyama, M., and Kunugi, T., *J. Catal.* **61,** 7 (1980).
18. Cant, N. W., and Bell, A. T., *J. Catal.* **73,** 257 (1982).
19. Duncan, T. M., Winslow, P., and Bell, A. T., *J. Catal.* **95,** 305 (1985).
20. Bennett, C. O., *Catal. Rev.* **13,** 121 (1976).
21. Graham, W. R. C., and Lynch, D. T., *Surf. Sci.* **187,** L633 (1987).
22. Graham, W. R. C., and Lynch, D. T., *AIChE J.* **33,** 792 (1987).
23. Boudart, M., "Kinetics of Chemical Processes." Prentice–Hall, Englewood Cliffs, NJ, 1968.
24. Che, M., and Bennett, C. O., "Advances in Catalysis" (D. D. Eley, H. Pines, and P. B. Weisz, Eds.), Vol. 36, pp. 55–172. Academic Press, San Diego, 1989.
25. Zhou, X., and Gulari, E., *J. Catal.* **105,** 499 (1987).